# DETECTOR FOR ROCKET MEASUREMENTS
# OF THE DIRECT SOLAR LYMAN-ALPHA RADIATION

**Veneta Guineva[1], Georg Witt[2], Jorg Gumbel[3], Mikhail Khaplanov[3], Rolf Werner[1], Jønas Hedin[3], Slaveyko Neychev[4], Boyan Kirov[5], Luydmil Bankov[1], Pavlin Gramatikov[4], VeselinTashev[1], Mikhail Popov[1], Kenneth Hauglund[6], Gudmund Hansen[6], Jørgen Ilstad[6], Halgeir Wold[6]**

[1]*Solar-Terrestrial Influences Laboratory - Bulgarian Academy of Sciences, Stara Zagora Department*
[2]*Department of Earth Sciences, The Hebrew University (HUJI), Jerusalem, Israel;*
[3]*Atmospheric Physics Group at the Department of Meteorology (MISU), Stockholm University*
[4]*Space Research Institute - Bulgarian Academy of Sciences*
[5]*Solar-Terrestrial Influences Laboratory - Bulgarian Academy of Sciences*
[6]*Andøya Rocket Range, Andenes, Norway*
*e-mail: v_guineva@yahoo.com*

*Key words: Lyman-alpha detector, direct solar radiation,rocket measurements*

*Abstract. The detector of solar Lyman-alpha radiation, manufactured in the Stara Zagora Department of the Solar-Terrestrial Influences Laboratory (STIL)is designed for rocket measurements. Its basic part is an ionization camera, filled in with NO. A 60 V power supply is applied to the chamber. The produced photoelectric current from the sensor is fed to a 2 channels amplifier, providing analog signal.*

*The characteristics of the Lyman-alpha detector were studied. It passed successfully integration test in the HotPay I payload, test of the 4 channels (2 data channels and 2 additional ones for the temperature and power supply monitoring) after connection to the TM with external and internal power, vibration and temperature tests and the results showed that the so-designed instrument could be used in rocket experiments to measure the Lyman-alpha flux.*

*From the measurements of the detector, the Lyman-alpha vertical profile can be obtained. The forthcoming scientific data analysis could include radiative transfer simulations, $O_2$ density, atmospheric power and temperature profiles retrieval as well as co-analysis with other parameters, measured at the same time and study of the processes in the examined region.*

*The detector design appertained to ASLAF project (Attenuation of the Solar Lyman-Alpha Flux), a scientific cooperation between STIL-Bul. Acad. Sci., Stara Zagora Department and the Atmospheric Physics Group at the Department of Meteorology (MISU), Stockholm University, Sweden. The joint project was part of the rocket experiment HotPay I, in the ALOMAR eARI Project, EU's 6th Framework Programme, Andøya Rocket Range, Andenes, Norway (Project HP11_VeGi).*

*The project is partly financed by the National Science Fund, Bulgarian Ministry of Education and Science (Project NoNZ-1515/05).*

**Introduction.** The Lyman-alpha ($L_\alpha$) radiation is of great importance of the atmosphere. It influences all the processes in the mesosphere and near the mesopause. The object of this paper is to describe an instrument, the Lyman-alpha detector (ASLAF) designed for measurements of the direct $L_\alpha$ radiation penetrating in the atmosphere, during the HotPay I experiment. The HotPay project is a part of the ALOMAR (Arctic Lidar Observatory for Middle Atmosphere Research) eARI Project of Andøya Rocket Range (ARR), Andenes, Norway, through EU's 6th Framework Programme. Two rocket launches have been envisaged: HotPay I and II. Studies of the middle atmosphere in the 60 – 110 km altitude range (HotPay I) and of the ionosphere and the aurora up to 300 km height (HotPay II) have been planned. A number of projects have been approved for the two rocket launches. The project ASLAF (Attenuation of the Solar Lyman-Alpha Flux) was one of these projects. It has been approved for the summer launch HotPay I in 2006. ASLAF was a joint project, based on the scientific cooperation between the Solar-Terrestrial Influences Laboratory (STIL), Bulgarian Academy of Sciences, Stara Zagora Department and the Atmospheric Physics Group at the Department of Meteorology (MISU), Stockholm University, Sweden.

The HotPay1 was launched July $1^{st}$ 2006, with a selected group of European scientific instruments onboard. The rocket caught unbalance and broke apart the rocket motor/payload section at flighttime about 7 – 8 seconds. The payload fell in the ocean about 80 sec. later. An external investigation was performed by DNV (Det Norske Veritas). The analyses showed that the joint between the rocket motor and the payload was weak. But housekeeping systems performed well and TM information was received from all instruments during the shortened flight. The payload was well balanced. A repetition of the HotPay I rocket experiment would give a chance to use the newly developed detector and to complete the scientific program.

**Peculiarities and importance of the Lyman-alpha radiation, advantages of the rocket measurements.** The basic goal of ASLAF was the measurement of the direct solar $L_\alpha$ radiation. The resonance transition $^2P$-$^2S$ of the atomic hydrogen (Lyman-alpha emission) is the strongest and most conspicuous feature in the solar EUV spectrum. It is one of the main characteristics of the solar radiation together with F10.7 MHz and, therefore it is the object of regular satellite and rocket measurements (Chamberlain, 1978; Marov, Kolesnichenko, 1987; Willson, 1990; Woods et al., 1995; Woods et al., 2000).

Due to the favorable circumstance, that the Lyman-alpha wavelength coincides with a minimum of the $O_2$ absorption spectrum, the direct Lyman-alpha radiation penetrates down to altitudes around 70 km for zenith sun (Woods et al., 1995; Kockarts, 2002).

Due to the relatively high intensity of the $L_\alpha$ emission and its comparatively deep penetration in the earth atmosphere it is the main source of energy deposited in the mesosphere. Therefore, the knowledge of the $L_\alpha$ radiation and its variation is important for many investigations of the middle and upper atmosphere (Woods, Rottman, 1997; Woods, Tobiska et al., 2000). The $L_\alpha$ study leads to a better understanding of the chemistry in the region mesosphere – low thermosphere, to including new chemical processes and transport mechanisms in the models. $L_\alpha$ influences the atmospheric structure and especially the D-region, allowing the determination of the H content in the atmosphere (Bishop, 2001; Kockarts, 2002).

Frequent in situ measurements of the $L_\alpha$ profile are necessary so as to understand all occurring processes in detail. For example, the origin and the structure of the noctilucent clouds (NLC), typical for the summer mesosphere at high latitudes are not yet fully clarified. It has been proposed that these clouds are the indicators of long-term changes in the upper atmosphere (Thomas, Olivero, 2001). The vertical structure of NLC, the dynamics, concentration and dimensions of the ice particles inside them are investigated (Gumbel, Witt, 1998). The generation, the evolution and the eventual sublimation of NLC, taking into account the influence of the solar $L_\alpha$ radiation, have been modeled and their influence on the chemistry of $O_2$, $O_3$ and H is studied by Murray and Plane (2004). The influence of the mesospheric ionization level, connected with the changes of the solar $L_\alpha$ radiation and the precipitating particles has been studied. The $L_\alpha$ change during the solar cycle together with the increase of methane in the atmosphere leads to long-term changes in the water vapour content in the mesosphere (Chandra et al., 1997).

The $L_\alpha$ attenuation in the earth atmosphere is modeled for different seasons and geographical latitudes, taking into account different processes: the $O_2$ absorption and its temperature and wavelength dependence, the multi-resonance scattering from atomic hydrogen and the related Doppler effect by Reddmann and Uhl (2002).

Rocket sounding is the basic method to study the mesosphere and the low thermosphere. The aerodynamic effects in rocket flights have been modeled and investigated by Gumbel (2001) in order to avoid errors in rocket in situ measurements, due to perturbations, as a result of the gas flux around the rocket.

Using rocket observations of the attenuation of the solar $L_\alpha$ radiation, registered by ionization chambers, the pressure, density and temperature in the mesosphere can be derived by traditional methods, described by Thrane et al. (1974), Thrane, Johannessen (1975), Thrane et al. (1977), Vardavas, Carver (1984).

The interaction of the Lyman-alpha radiation with the atmospheric constituents ionises the NO molecules, thus giving rise to the ionospheric D-layer and produces the water vapour photolysis, one of the main $H_2O$ loss processes. The Lyman-alpha radiation transfer depends on the resonance scattering from the hydrogen atoms in the atmosphere and on the $O_2$ absorption. Since the Lyman-alpha extinction in the atmosphere is a measure for the column density of the oxygen molecules, the atmospheric temperature profile can be calculated thereof.

The importance of the $L_\alpha$ penetration in the thermosphere and mesosphere as a main source of energy input and its connection with the $O_2$ concentration and the temperature as well with all processes in these regions is known long ago. At the same time, lots of ambiguities in our concepts for the chemical and physical processes in the mesosphere, low thermosphere and, in particular near the mesopause, have been found out. Such not fully clarified questions are, for example, the influence of $L_\alpha$ on the trace gases, the role of $CO_2$ and $CH_4$ on the temperature distribution, the origin and structure of NLC and the properties of their constitutive ice particles (Kockarts, 2002; Thomas, Olivero, 2001; Chandra et al., 1997; Roble, Dickinson,

1989; Thomas et al., 2003; Von Zahn, 2003). That is why the $L_\alpha$ measurements and the study of the middle atmosphere processes are important features to be investigated.

**Principal scheme and functioning of the solar Lyman-alpha detector.** The solar Lyman-alpha detector was designed to record the direct solar radiation flux in the EUV, at the $L_\alpha$ wavelength range, from 50-60 to 110 km. After a preliminary agreement, the measuring device was manufactured in the Stara Zagora Department of STIL. A work model and a flying one were produced. The principal scheme of the instrument is shown in Fig.1. The EUV solar $L_\alpha$ detector had 3 basic parts: sensor, electronics and power supply. The sensor was an ionization cha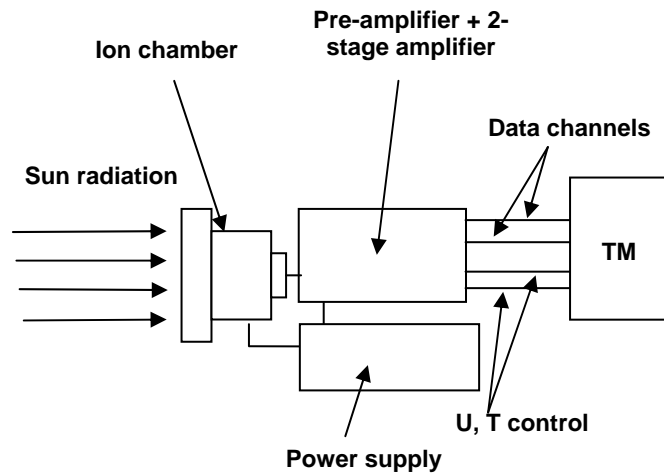mber. The electronics included a pre-amplifier and a 2-stage amplifier. The ionization chamber was filled with NO. Its window let pass the radiation that was of interest of us. The working voltage was applied to the central electrode-collector. The role of the other electrode was executed by the chamber walls. $L_\alpha$ ionized NO and thanks to the existing potential a weak current was produced. This current was amplified many times in the pre-amplifier and passed through the amplifier, where it got amplification with different coefficient in the different stages (x1 and x10). Finally the analog signal was fed to the telemetry as voltage in the range 0-5 V. Two additional channels to monitor the temperature and the power supply to the chamber were foreseen except the two data channels. The role of the power supply was to transform and fed the needed power supply to the ionization chamber and the electronics plates.



**Fig. 1.** *Principal scheme of the Lyman-alpha detector*

**Ionization chamber.** The ionization chamber is the basic element of the $L_\alpha$ detector. The principal structure of similar ionization chambers for the UV region is described, for example, in Stober et al. (1963), Carver, Mitchel (1964), Masuoka, Takanori (1974), Thrane et al., (1975). In our experiment, an ionization chamber of the Artech Corporation was used of the same kind as the one which turned to be efficient in the Thrane experiment (Thrane et al., 1975). The cell was made from copper. Its weight was about 50 g, and its maximal dimensions were diameter 30 mm, length 36 mm, and full length with the gas-filling tubule (32 mm) – 68 mm. It was furnished with $MgF_2$ window of 8 mm diameter and filled with NO. The spectral sensitivity of such chambers extends from 105 nm to 135 nm with a quantum efficiency Q of 40% ÷ 60% for voltages 25V ÷ 150V.

The choice of the ionization chamber position was made in accordance with the launch parameters of HotPayl. It was decided the angle between the chamber and the vertical rocket axis to be 55°, thus anticipating best illumination from the Sun.

Measurements have been carried out at MISU to specify the properties of the ionization chamber and to estimate the available power supply and NO pressure. A H lamp was used as $L_\alpha$ source. The obtained current through the ionization chamber at different conditions – power supply and pressure at the same $L_\alpha$ flux, is shown in Fig.2. The NO pressure, corresponding to optical depth 1, was theoretically evaluated 10 mb. Work values U = 60 V and p = 20 mb were chosen. The produced current at 60 V was stable towards changes in the power supply. Possible changes of ±1 V in the power supply were agreed. It was estimated, that at pressure 20 mb of the NO gas 86% of the penetrated $L_\alpha$ radiation in the chamber must be absorbed. At the chosen incident radiation, and U and p values the produced current reached nearly the maximal possible value.
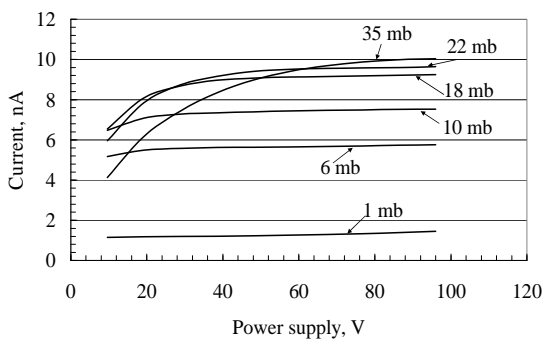


**Fig.2.** *Current through the ionization chamber, registered at different conditions – power supply and NO pressure*

**Electronics.** The electronics amplifier had to possess high quality characteristics: high sensitivity, high amplification coefficient, large dynamic range, high transformation accuracy and good stability against temperature changes. The circuitry of the electronic amplifier is shown in Fig.3.

The current from the ionization chamber passed

through a jointly-fixed low-noise pre-amplifier (Section A1 in Fig.3). It was situated close to the ionization chamber in order to avoid the hum noises.
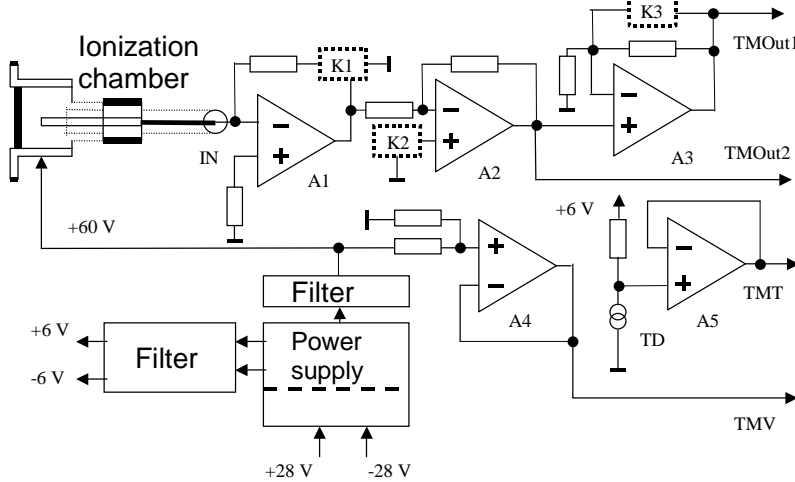


**Fig. 3.** *Circuitry of the electronic amplifier. It consists of the following Sections: A1 - pre-amplifier and current-voltage converter; A2 – scaling and correcting amplifier; A3 – amplifies the signal 10 times; A4 – monitors the ionization chamber power supply; A5 – monitors the temperature.*

The maximal photoelectric current to measure at the atmospheric boundary was evaluated to be 20 nA (Thrane et al., 1975). We decided a maximal measurement current of 15 nA in the electronics design. This value corresponds to the current at the border of the atmosphere, direct Sun, and Q=60% of the ionization chamber. We assumed that with this value the instrument wouldn't reach saturation and could be calibrated in absolute units using simultaneous satellite measurements of $L_\alpha$ outside the atmosphere.

The range 0-15 nA could be covered by a single channel thanks to the contemporary electronics elements. We decided to use 2 channels (2-stage amplifier) in order to register in detail the weaker signals. The amplifications were x1 for the 15 nA channel(Section A2 in Fig.3) and x10 for the 1.5 nA one (Section A3 in Fig.3). The two channels worked simultaneously and transferred analog signal in the range 0-5 V to the TM. A measurement frequency of 1000 Hz was envisaged. Besides, two sub-commutated channels to monitor the sensor conditions: the power at the chamber (60V±1V) (Section A4 in Fig.3) and the temperature (Section A5), were included.

**Power supply.** The power supply satisfied the following requirements: it kept its full work ability at changes of the internal board power from 20 V to 34 V, the nominal board power being 28 V; ensured stabilized secondary voltages and currents: +6V/25mA, -6V/ 25mA and +60V(±1V) /1mA; the starting current amplitude in the board circuit didn't surpass 3 A; ensured galvanic denouement between the board circuit and the secondary voltages.

**ASLAF design and dimensions.** Most of the instruments included in the HotPayl project, were foreseen to be positioned in the nosecone, on the top deck. The Lyman-alpha detector ASLAF was on the nosecone deck, too.

The mechanics and electronics of the instrument were designed in such a way as it fitted well and completely in the small remaining free space in the nosecone. The mechanics and electronics design of the Lyman-alpha detector were made simultaneously and coordinated.

The Lyman-alpha detector ASLAF had complicated form with maximal dimensions 105x60x90 mm and weight 498 g. Its compactness and low weight make it expedient for rocket measurements. The final appearance of ASLAF is presented in Fig.4.
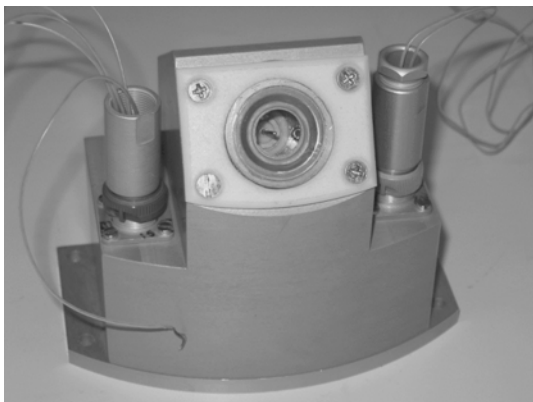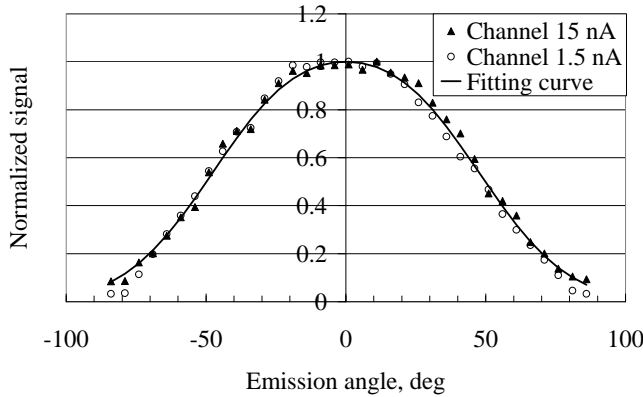


**Fig. 4.** *Final design of the Lyman-alpha detector*

According to the final design of ASLAF, the instrument body was produced from monolithic piece of alluminium, ensuring maximal strength of the construction. The whole instrument, including the amplifier and the power supply, was hold in one box in the purpose to avoid the noise. The box form was chosen in such way, that the whole free space of the circle (the upper deck) was used. The ionization chamber was situated perpendicularly to the neighbour instrument, under 55° towards the vertical rocket axis. This assured 180° field of view and the maximal possible illumination by the Sun at every rocket spin. The components inside the instrument body were situated in such a way, that the output of the ionization chamber was connected directly to the entrance of the electronics amplifier in order to avoid the induced noise. The electronics plates were shielded, grounded and electrically isolated from the instrument body to avoid external noise. The ionization chamber was isolated from the plates

shields and the instrument body, too.

A work and a flying model of the Lyman-alpha detector ASLAF were produced. The work model was used for the first test and calibrations, and conclusions how to improve its parameters were taken. The decisions were applied to the flying model, and very good results were obtained.

**Characteristics of the Lyman-alpha detector.** The ionization chamber is sensitive to the incidence angle of the radiation, the window effective surface being proportional to the cosine of the angle to the Sun. A maximal output is obtained, when the window is fully illuminated, and the optical axis points straightwards to the Sun. The dependence of the instrument response on the angle of radiation incidence was studied. The obtained result is shown in Fig.5. The dependence is symmetric towards the perpendicular to the chamber window and one and the same for both channels. It is wider than a Gauss curve. A curve, fitting well the obtained dependence was constructed as the sum of two Gauss curves displaced one towards the other:

**Fig. 5.** Dependence of the measured signal on the incident radiation angle for both ASLAF channels. The obtained fitting curve is drawn in.

$$y = \frac{e^{-a(x-b)^2} + e^{-a(x+b)^2}}{c}$$

The relative error using this curve for measurement analysis was obtained. It doesn't exceed 4% up to $\pm 50°$ and 10% up to $\pm 70°$.

The Lyman-alpha detector response to the H lamp emission was studied. Linear signal depending on the emission intensity was obtained from both channels. The signal ratio could be considered 10.6 from 30 mV to 4.2 V in the channel 1.5 nA range.
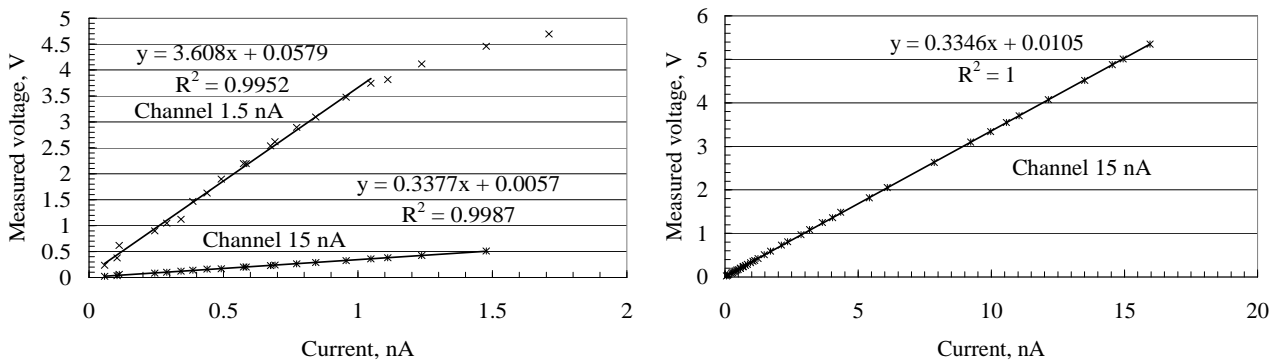
*Fig. 6. Dependence of the measured voltage on the produced electric current for both channels*

The dependence of the measured voltage on the flown electric current was linear for both data channels and constant signal ratio was obtained. The results are shown in Fig.6.

The bias signal was very low: practically 0 for the 15 nA channel and x100$\mu$V for the 1.5 nA channel.

Noise and signal test measurements were implemented and gave very good results. When all instruments were on board and the internal power was switched on, the noise in channel 15 nA was practically zero, and the one in channel 1.5 nA was very low, with average value of 2.6 mV, what is near the sensitivity threshold.

**Conclusions.** A state-of-the-art instrument - Lyman-alpha detector (ASLAF) to record the attenuation of the direct Lyman-alpha radiation in the atmosphere was designed and a work model and a flying one were manufactured. All conditions were carefully considered and the general parameters influencing the measurements were estimated on the basis of the existing theory as well as on the results of previous experiments. The mechanics and electronics of the instrument were designed to fit the space allotted on the upper deck of HotPayl, under the nosecone. It is maximum compact and light. The position and the operating conditions of the ionization chamber were chosen on the basis of planned experiments and theoretical estimates. A set of tests were performed in order to study the characteristics of the ionization chamber and the electronics and their response to the expected signal.

ASLAF passed successfully all tests performed before a rocket launch. All measured characteristics were within the borders of the expected values and with very good quality. There are two measuring channels with ranges 1.5 nA and 15 nA, characterized with linearity, constant data ratio between them and

low noise signal. The two channels monitoring the power supply to the ionization chamber and the temperature operated well. The power supply to the ionization chamber remained stable, 60V, with deviations from this value less then 1V.

The device is of very good quality and it is expedient to be used in rocket experiments for measuring the Lα flux.

**References:**

1. B i s h o p  J. 2001. Thermospheric Atomic Hydrogen Densities and Fluxes from Dayside Lyman $\alpha$ Measurements. Journal of Atmospheric and Solar-Terrestrial Physics 63, 331-340.
2. B r e m e r  J., P. H o f f m a n n, R. L a t t e c k, W. S i n g e r. 2003. Seasonal and Long-Term Variations of PMSE from VHF Radar Observations at Andenes, Norway. Journal of Geophysical Research (Atmospheres) 108 (I.D8), PMR 5-1, citeID 8438, DOI.
3. C a r v e r  J.H.,  P. M i t c h e l. 1964. Ionisation Chambers for the Vacuum Ultra-Violet. J.Sci. Instrum. 41, 555-557.
4. C h a m b e r l a i n  J. 1978. Theory of Planetary Atmospheres. Academic Press.
5. C h a n d r a  S., C.H. J a c k m a n, E.L. F l e m i n g, J.M. R u s s e l l. 1997. The Seasonal and Long Term Changes in Mesospheric Water Vapour. Geophysycal Research Letters 24 (I.6), 639-642.
6. G u m b e l  J., G. Witt. 1998. In Situ Measurements of the Vertical Structure of a Noctilucent Cloud. Geophysycal Research Letters 25 (I.4), 493-496.
7. G u m b e l  J. 2001. Aerodynamic Influences on Atmospheric in situ Measurements from Sounding Rockets. Journal of Geophysical Research 106 (NA6), 10553-10563.
8. K o c k a r t s  G. 2002. Aeronomy, a 20th Century Emergent Science: the Role of Solar Lyman Series. Annales Geophys. 20, 585-598.
9. M a r o v  M.Ya., A. K o l e s n i c h e n k o. 1987. Introduction to the Planetary Aeronomy. Moscow. Nauka (in Russian).
10. M a s u o k a T., O. T a k a n o r i. 1974. Lyman-alpha Detector with $MgF_2$ Window. Rev. Sci. Instrum. 45, 1012-1014.
11. M u r r a y  B.J., J.M.C. P l a n e. 2004. Modelling the Impact of Noctilucent Cloud Formation on Atomic Oxygen and Other Minor Constituents of the Summer Mesosphere. Atmospheric Chemistry and Physics Discussions 4, 7181-7216.
12. P a n c h e v a  D., R. S c h m i n d e r,  J. L a s t o v i c k a.  1991. 27-day Fluctuations in the Ionospheric D-Region. Journal of Atmospheric and Terrestrial Physics 53 (ISSN 0021-9169), 1145-1150.
13. R e d d m a n n  Th., Uhl, R. 2002. The Solar Hydrogen Lyman-alpha Photon Density within the Mesosphere. EGS XXVII General Assembly, Nice, 21-26 April, Abstract #2186.
14. R o b l e  R.G., R.E. D i c k i n s o n. 1989. How Will Changes in Carbon Dioxide and Methane Modify the Mean Structure of the Mesosphere and Termosphere?. Geophysical Research Letters 16, 1441-1444.
15. S t o b e r  A.K., R. S c o l n i k,  J.P. H e n n e s. 1963. A Vacuum Ultraviolet Photoionization Detector. Applied Optics 2, 735-739.
16. T h o m a s  G.E., J. O l i v e r o. 2001. Noctilucent Clouds as Possible Indicators of Global Change in the Mesosphere. Advances in Space research 28 (I.7), 937-946.
17. T h o m a s  G.E., J.J. O l i v e r o, M. D e L a n d,  E.P. S h e t t l e. 2003. A Response to the Article by U. von Zahn, Are Noctilucent Clouds Truly a "Miner's Canary" of Global Change?. EOS, Transactions, American Geophysical Union, 84(36), 352-353.
18. T h r a n e  E.V., I. N y b e r g, B. N a r h e i m. 1974. Measurements of the Extinction of Solar Hydrogen Lyman-$\alpha$ in the Mesosphere. Internal Report E-230, Norwegian Defense Research Establishment (FFI), Norway.
19. T h r a n e  E.V., A. J o h a n n e s s e n. 1975. A Measurement of the Extinction of Solar Hydrogen Lyman-$\alpha$ Radiation in the Summer Arctic Mesosphere, Journal of Atmospheric and Terrestrial Physics 37, 656-661.
20. T h r a n e  E.V., O. H a g e n, F. U g l e t v e i t.  1977. Rocket Measurements of Mesospheric Density, Pressure and Temperature. Internal Report E-269, Norwegian Defense Research Establishment (FFI), Norway.
21. V a r d a v a s  I.M., J. H. C a r v e r. 1984. Comments on the Newton-Raphson Method for Obtaining Temperature Profiles from Radiative-Convective Models. Planetary and Space Science 32 (I.7), 803-807.
22. V o n  Z a h n U. 2003. Are Noctilucent Clouds Truly a "Miner's Canary" of Global Change?. EOS, Transactions, American Geophysical Union, 84(28), 261-268.
23. W i l l s o n  R.C. 1990. Solar Irradiance Variability During Solar Cycles 21 and 22. In NASA, Goddard Space Flight Center, Climate Impact of Solar Variability, 279 (SEE N91-12456 03-92).
24. W o o d s  Th.N., G.J. R o t t m a n, O.R. W h i t e, J. F o n t e n l a, E.H. A v r e t t. 1995. The Solar $L_{y\alpha}$ line profile. Astrophysical Journal 442, 898-906.
25. W o o d s  Th.N., W.K. T o b i s k a, G.J. R o t t m a n, J.R. W o r d e n. 2000. Improved Solar Lyman alpha Irradiance Modelling from 1947 through 1999 Based on UARS Observations. Journal of Geophysical Research 105 (I.A12), 27195-27216.
26. W o o d s  Th.N., G.J. R o t t m a n. 1997. Solar Lyman alpha Irradiance Measurements During Two Solar Cycles. Journal of Geophysical Research 102 (I.D7), 8769-8780.
27. W o o d s  Th.N., W.K. T o b i s k a, G.J. R o t t m a n, J.R. W o r d e n. 2000. Improved Solar Lyman alpha Irradiance Modelling from 1947 through 1999 Based on UARS Observations. Journal of Geophysical Research 105 (I.A12), 27195-27216.